Histol Histopathol (2015) 30: 1499-1512

http://www.hh.um.es

Histology and Histopathology

Cellular and Molecular Biology

Development and preclinical evaluation of a new galactomannan-based dressing with antioxidant properties for wound healing

Begoña Castro[1], Teodoro Palomares[2], Iker Azcoitia[1], Felix Bastida[3], Maite del Olmo[1], Javier J. Soldevilla[4] and Ana Alonso-Varona[2]

[1]Histocell, Bizkaia Science and Technology Park, Derio, Bizkaia, [2]Faculty of Medicine and Dentistry, University of the Basque Country (UPV/EHU), Leoia, Bizkaia, [3]ArtinVet, Bizkaia Science and Technology Park, Derio, Bizkaia and [4]Hospital de San Pedro, Servicio Riojano de Salud, La Rioja, Spain

Summary. We describe a novel wound dressing (HR006) with two components: a lyophilized matrix of the galactomannan from *locust bean gum* (LBG) and an antioxidant hydration solution (AH_{sol}) containing curcumin and N-acetyl-L-cysteine (NAC). Physico-structural analyses of the LBG matrix revealed homogeneous interconnected pores with high absorbing capacity showing excellent properties for moist wound care (MWC). In an *in vitro* oxidative stress fibroblast injury model, the AH_{sol} showed relevant protective effects reducing intracellular reactive oxygen species (ROS) production, rescuing cell viability, and regulating expression of inflammation-related genes (COX-2, TNF-α, IL-1α, IL-1β). The new dressing showed good biocompatibility profile as demonstrated by cytotoxicity, hemocompatibility, and skin irritation tests. Moreover, in an *in vivo* skin wound model in pigs, this dressing enhanced the production of healthy and organized granulation tissue and re-epithelization. In summary, HR006 exhibits significant antioxidant activity, good biocompatibility, and excellent repair capabilities improving tissue remodeling and the healing of wounds.

Key words: Galactomanan-based matrix, Antioxidant wound dressing, Skin wound healing, Oxidative stress

Offprint requests to: Dr. Ana Alonso-Varona, Department of Cell Biology and Histology, School of Medicine and Dentistry, University of the Basque Country, E-48940 Leioa, Bizkaia, Spain. e-mail: ana.alonsovarona@ehu.es

DOI: 10.14670/HH-11-646

Introduction

Skin wounds in humans, such as cuts, burns, lacerations or ulcers (pressure, venous leg, or diabetic foot) are a significant clinical problem and an economic burden for the majority of healthcare systems (Drew et al., 2007; Sen et al., 2009; Hopman et al., 2013). The management of wounds has recently improved significantly, including regenerative therapy (skin replacement, cell therapies), negative pressure wound therapy, hyperbaric oxygen therapy, electromagnetic or ultrasound therapies, and innovative therapies for moist wound care (MWC) (Günter and Machens, 2012; Dreifke et al., 2015; Kirsner et al., 2015). Because several of these new therapies have either not been thoroughly tested or have not shown an improvement over traditional wound treatments in clinical trials (Murphy and Evans, 2012; Smith et al., 2013), the development of new materials and therapies for active wound healing is exceedingly important.

Wound healing is a complex process arranged in three overlapping but distinct phases: inflammatory, proliferative and tissue remodeling (Schreml et al., 2010). Therapies must take into account these stages in order to facilitate a more physiological and orchestrated healing. In this sense, MWC allows us to create an optimal environment, where proliferating and migrating cells interact with each other via bioactive molecules, such as growth factors, conducting a coordinated healing process.

Today, treatments with advanced dressing products for MWC include specially designed materials with appropriate morphological and physical characteristics

(sponges, foams, transparent films, hydrocolloids, calcium alginates, hydrogel dressings, etc.). These materials can be used alone or in combination with many different types of active ingredients, such as antibiotics or compounds with antimicrobial activity (silver), anti-inflammatories, anesthetics or analgesics (lidocaine, ibuprofen), growth factors (EPO, EGF, FGF, KGF, PDGF), plant healing factors (aloe vera) or other natural ingredients (honey) that can all, in theory, help in the healing process (Percival et al., 2008; Wolcott et al., 2008; Günter and Machens, 2012; Tsala et al., 2013; Jull et al., 2015). However, even with these new treatments, often a healing delay occurs leading to chronification of wounds, which may be due to a failure in some aspects of the repair process. Among them, several studies have shown that oxidative stress during the inflammatory phase of wound repair is a significant factor in healing delay (Schäfer and Werner, 2008). Pro-inflammatory cytokines (ie, TNF-α, IL-1α) and reactive oxygen species (ROS), such as •O2-, •OH, and H_2O_2, secreted mainly by neutrophils and macrophages, are present at the site of injury and in the wound's exudates (Sen and Roy, 2008; Vermeij and Backendorf, 2010; Wagener et al., 2013). ROS are necessary as a defense mechanism against pathogens and also as intermediate molecules in many signal transduction and homeostasis processes in the cell (Finkel, 2011; Jiang et al., 2011; Ray et al., 2012). Moreover, physiological-steady state levels of these molecules are also critical for wound healing and remodeling of tissues (Gauron et al., 2013). However, since ROS have potent oxidizing capabilities, when secreted out of control, they can damage DNA, lipids, and proteins causing oxidative stress in the wound bed and arresting or delaying the healing process, ultimately leading to chronification of the wound (Roy et al., 2006). Therefore, the use of a wound dressing that can exert the appropriate antioxidant effect on wound exudates and maintain humidity and ROS balance should help resolution of wounds (Sen, 2009; Fitzmaurice et al., 2011).

In this manuscript, we report the development of a new antioxidant dressing for MWC (HR006). This product includes two components: i, an absorbent matrix composed of a galactomannan from vegetal origin (*locust bean gum*, LBG) that provides a porous structure, and ii, an antioxidant hydration solution (AH_{sol}), composed of curcumin and N-acetyl-L-cysteine (NAC), that gives adequate moisture to the wound bed. LBG had previously been used for the treatment of internal ulcers, but we developed a new method for producing non-resorbable natural LBG based matrices with antioxidant properties that showed high exudate absorbing capacity for the treatment of skin wounds. In an *in vitro* oxidative stress injury model, based on the exposure of human fibroblasts to H_2O_2, we showed that AH_{sol} components exert a marked protective effect, reducing the ROS levels and regulating the expression of inflammation-related genes (COX-2, TNF-α, IL-1α, IL-1β). In addition, HR006 components were not cytotoxic and demonstrated good biocompatibility. Finally, *in vivo* studies in pigs showed a more orderly transition between the inflammatory, proliferative, and remodeling phases of wound healing.

Materials and methods

Synthesis and characterization of the antioxidant wound dressing (HR006)

Synthesis of the matrix

Galactomannan from LBG (5-7% w/v; Carob. S.A, Mallorca, Spain) was solubilized in acid aqueous solution under constant stirring at high temperature. Galactomannan matrices (hydrogels) were obtained by cross-linking monomers in glutaraldehyde. Hydrogels were then washed for 2 h with a 5% (w/v) solution of sodium bisulfite and, for an additional 2 h, with deionized-distilled water until no traces of glutaraldehyde could be detected (spectrophotometer at 235 nm and 280 nm). Hydrogels were dried by lyophilization (3D galactomannan matrix). For some *in vitro* cellular experiments, hydrogels must be produced as 2D matrices (2D film) by drying the matrices with heat at 50°C until weight was constant instead of by lyophilization. Hydrogels were either dried by heat (2D galactomannan film) or by lyophilization (3D galactomannan matrix).

Scanning electron microscopy of the matrix

Cross-section morphology of the lyophilized matrix was analyzed using a Hitachi S-4800 scanning electron microscopy (SEM; Hitachi, Tokyo, Japan) at accelerating voltage of 15 kV and different magnifications. All samples were pre-coated with a conductive layer of sputtered gold.

Equilibrium water content of the matrix

To assess the equilibrium water content (EWC) of the matrix following ISO 13726:2002, one cm^2 samples were used. The equilibrium water from matrices of three different batches of HR006 was calculated as the ratio of solvent to dry sample following the formula: $EWC=(Ws-Wd) / Wd$ where Wd is the weight of the dry sample, and Ws is the weight of the swollen sample in equilibrium.

Ash content of the matrix

Inorganic residual content is related to the impurities in a product. A matrix sample was weighed and burnt at temperatures above 500°C, and residual matter was weighted after cooling in a desiccator. Ash content was calculated following the formula: $\%Ash=(W_{ash} / W_{initial}) \times 100$, where W_{ash} is the weight of the remaining ash after the matrix is burnt, and $W_{initial}$ is the weight of the matrix at the beginning.

In vitro cytotoxicity of the matrix

Experiments were done following ISO standard 10993-5:2009 Annex C. Liquid extract of the LBG matrix was obtained by incubating it with culture media at 37°C for 24 h, according to ISO standard 10993-12:2007. Percent viability was calculated as follows: $\%\ Viability = (OD\ Sample / OD\ Negative\ control) \times 100$, where OD is the absorbance value at 550 nm of the dissolved formazan crystals result of the metabolization of the MTT dye by live cells.

To further analyze cell viability when in contact with cross-linked galactomannan, due to technical reasons, instead of using 3D matrices, we produced 2D matrices (film) and determined the degree of cell adhesion and viability of human fibroblasts on its surface. LBG film was sterilized using a UV lamp for 1 hour and incubated for 30 min in culture media. After discarding this media, fibroblasts were seeded onto the 2D film and grown for 48 h at 37°C. Cells were stained with calcein AM following manufacturer's protocol (Life Technologies, Carlsbad, USA). Images, obtained with an inverted fluorescence microscope (Olympus IX51), show live cells stained green.

Selection of the components of the antioxidant hydration solution (AH_{sol})

To partially hydrate the matrix for optimal MWC, we designed a hydration solution with antioxidant properties. Of the many potential antioxidant molecules approved for medical use, we selected curcumin and NAC (Sigma-Aldrich, St. Louis, MO, USA). Curcumin is a well known antioxidant with dermal healing properties, and NAC has strong antioxidant capacity and low toxicity (Morley et al., 2003; Akbik et al., 2014). For this study we use a range of 0.5-100 μM for curcumin and 0.05-10 mM for NAC.

Antioxidant capacity of HR006 components

The oxygen radical absorbance capacity assay (ORAC) was used for screening antioxidant capacity of the selected molecules LBG, curcumin, and NAC as previously described (Ou et al., 2001). This assay is based on the oxidation of fluorescein (Sigma-Aldrich) by peroxyl radicals produced by the free radical initiator 2,2'-azobis-2-methyl-propanimidamide, dihydrochloride (AAPH; Sigma-Aldrich). Oxidation of the probe reduces its fluorescence. In the presence of antioxidants, the probe's oxidation is inhibited, and thus no decrease in fluorescence takes place. Data were normalized in relation to time zero values of the control wells.

Oxidative stress model

In vitro oxidative stress

Human neonatal fibroblasts, obtained from Histocell S.L. cell type collection were cultured at 37°C and 5% CO_2 in DMEM (Sigma-Aldrich) supplemented with 10% fetal calf serum (Biochrom AG, Berlin, Germany), 100 U/mL penicillin, 100 μg/mL of streptomycin, and 25 μg/mL of amphotericine B (Lonza, Maryland, USA). Fibroblasts at passage 2 to 5 were exposed to different concentrations of H_2O_2 for 1 h (Panreac, Barcelona, Spain). Oxidizing media were always added in relation to the number of cells and the surface of culture plate. After oxidation, media were removed, and cells were incubated in fresh culture media.

Cell viability and proliferation analyses

Cells were cultured in 96 well plates (4×10^3 cells/well). For morphological evaluation, images of control and oxidized fibroblasts were obtained in a phase contrast microscope (Olympus IX51, Tokyo, Japan). Viability and proliferation under different treatments were quantified incubating oxidized cells with MTT solution (Roche, Indianapolis, USA) in media (0.5 mg/mL) during 4 h. Formazan crystals were dissolved with solubilization solution (10% SDS in HCl 0.01M) during overnight incubation, and the optical density quantified spectrophotometrically (550 nm).

Intracellular ROS determination

Intracellular ROS levels were quantified using 2',7'-dichlorodihydrofluorescein diacetate (DCFH-DA; Molecular Probes, Oregon, USA) as a fluorescent probe. Fibroblasts were plated in 96 well tissue culture plates at 4×10^3 cells/well and incubated for 18 h. After this period, medium was removed and fresh medium with 10 μM DCFH-DA was added. Plates were incubated at 37°C for 30 min in the dark. Medium was then replaced with oxidizing media in the absence or presence of antioxidants. Fluorescence in the wells was measured every 5 min during 90 min (λ_{ex} 485 nm/λ_{em} 528 nm; Thermo Fisher Scientific Inc., Waltham, MA, USA).

Intracellular glutathione determination

Cellular glutathione (L-gamma-glutamyl-L-cysteinyl-glycine, GSH) concentrations were determined with monochlorobimane (mBCl), a probe that reacts specifically with GSH in living cells via GST to form a fluorescent derivative. Cells were plated in 96-well plates at 15×10^3 cells/well. After 18 h, cells were exposed to H_2O_2 for 1 h and the oxidizing media replaced by fresh medium. At specific times, cells were then washed and exposed to 100 μM mBCl in PBS for 15 min at 37°C in the dark and fluorescence was measured (λ_{ex} 380 nm/λ_{em} 465 nm). Since exposure to H_2O_2 can affect cell number and viability, data were always standardized to MTT cell viability data obtained from the same well.

Gene expression

mRNA from oxidized cells, treated or not with

AH_{sol}, was isolated using Total RNA isolation mini kit (Agilent, Santa Clara, CA, USA), and 1 μg of mRNA was used to generate first strand cDNA (Superscript TM III First-Strand Synthesis System kit; Invitrogen, Carlsbad, USA). Relative expression of genes related to inflammation and wound healing (COX-2, TNF-α, IL-1α, IL-1β) was measured with FAM labeled TaqMan Gene Expression Assay kits (assay numbers Hs00153133_m1, Hs01113624_g1, Hs00174092_m1, Hs01555410_m1; Applied Biosystem, Carlsbad, USA). Beta-actin (Hs01060665_g1; Applied Biosystem, Carlsbad, USA) was used as the internal control gene, because we have previously determined that its expression in human fibroblasts remains constant during oxidative stress. qPCR data were analyzed with the comparative C_T method ($-2\Delta\Delta C_T$) using the software SDS v1.4.1 (Applied Biosystem, Carlsbad, USA).

Biocompability of HR006

In vitro cytotoxicity

Media and conditions described above were used to culture murine fibroblasts cell line L929 (American Type Culture Collection, Manassas, VA, USA) for cytotoxicity experiments according to ISO standard 10993-5:2009 Annex C. To obtain HR006 fluid extract, the matrix was incubated with AH_{sol} and culture media (50:50), following ISO 10993-12:2007. Three different batches of HR006 were tested. Data were analyzed using the formula described earlier.

In vitro hemocompatibility

Hemocompatibility of three batches of HR006 was analyzed using the method of cyanmethemoglobin following ISO standard 10933-4:2002 Annex C. This method estimates the potential damage of a biomaterial to red cells by quantifying hemoglobin release. For colorimetric detection of hemoglobin, Drabkin reagent (Stanbio, Boerne, TX, USA) was used. Hemoglobin concentration was calculated according to a standard curve prepared with cyanmethemoglobin (Stanbio). Percent hemolysis was calculated with the following formula: *%Hemolysis*=[(*Sample hemoglobin-Negative control hemoglobin*) / (*Positive control hemoglobin - Negative control hemoglobin*)] × 100

In vitro irritation test

Skin irritation was analyzed in three batches of HR006 biomaterial. A validated irritation test (SkinEthic™ RHE "42bis", SkinEthic, Lyon, France) was used to analyze human skin irritation potential of HR006 following the manufacturer´s instructions. This method uses an *in vitro* reconstructed human epidermis (RHE) as a model equivalent to the human skin. Cell viability above 50% predicts a non irritancy potential of the tested substance.

In vivo experiments

Animal ethics committee

All animal experiments were done at the Autonomous University of Barcelona facilities and procedures were approved by regional authorities and Institutional Animal Care and Use Committee (DAAM #4230/CEEAH protocol #730). All procedures were performed according to the Guide for the Care and Use of Laboratory Animals and following European and Spanish Animal Welfare Laws.

Wound model in pigs

An acute excisional wound model in the pig was used to test the new antioxidant wound dressing HR006. Three Large White pigs weighing 24-50 kg were used after an acclimatization period of 1 week. Pigs were sedated (intramuscular azaperone at 4 mg/kg and ketamine at 10 mg/kg) and traqueally intubated. Analgesia was induced with intravenous buprenorfine (0.01 mg/kg), and anaesthesia was induced and maintained with propofol (4 mg/kg) and isoflurane (1,5-2%, oxygen). Before surgery, animals were treated with antibiotic (22 mg/kg cephalotin iv). Skin lesions (6×2 cm) that removed dermal and epidermal tissue were surgically generated in the dorsal area of each pig. All experiments included a control wound that was treated under MWC conditions with a commercial dressing. Test wounds were covered with hydrated HR006. All lesions, controls and tests, were then covered with a secondary wound dressing (hydrocolloid) to isolate and protect the skin lesions. Wound dressings were changed on days 3, 6, 10, 13, and 16. Macroscopic evaluation of tissue healing was performed throughout the experiment; lesions were measured at each time point, and the results expressed as the percentage of wound reduction with respect to control wound.

Histology and immunochemistry

Biopsies from control and HR006-treated wounds for histological evaluation were obtained at days 6, 10, and 16 from a region overlapping healthy tissue and wound. All skin biopsy samples were fixed in 10% neutral buffered formalin, routinely processed, and stained with hematoxylin and eosin (H&E). To further analyze the differences between HR006-treated and control wounds in relation to the phases of wound healing, biopsies from a representative pig were also stained with Masson's trichrome stain (standard laboratory procedure) or immunostained with antibodies to cytokeratins (Polyclonal Rabbit Anti-Cytokeratin, Wide Spectrum Screening, Dako, Carpinteria, CA, USA). For immunostaining, sections were first subjected

to a de-pigmentation treatment, and in order to avoid endogenous peroxidase activity, they were also incubated for 30 min with a 3% H_2O_2 solution in the dark. An antigen retrieval step was then done incubating sections 8 min at 37°C with 0.1% protease in PBS. Next, sections were incubated at 37°C for 1 h in 30% normal goat blocking serum in PBS, and incubated overnight at 4°C with antibodies against cytokeratins (1:10000; polyclonal rabbit anti-cytokeratin WSS, Z0622, Dako) diluted in 10% normal goat serum in PBS. Immunocomplexes were visualized with EnVision+ System-HRP (DAB) for rabbit primary antibodies (K4011, Dako).

Statistical analyses

GraphPad PRISM® (San Diego, CA, USA) was used for statistical analyses. Regression analysis was used for estimation of the IC50. Two variable data were compared using Student's t-test. ANOVA was used for assays with multiple variables, and the Bonferroni multiple comparison correction was applied when comparing individual treatments.

Results

Physico-chemical and biological characteristics of the lyophilized 3D matrix

To evaluate the physical and chemical characteristics of galactomannan-based matrix, the internal structure, absorption capacity, ash content, and antioxidant activity were examined. Scanning electron microcopy (SEM) showed an inner orderly structure of uniform interconnected pores with polyhedrical shapes, approximately of 200 μm in size (Fig. 1a-c). Water retention in hydrogels is related to the hydrophilic groups and cross-linking density as an opposing force to the solvation of the matrix. HR006's matrix absorption capacity was determined with the equilibrium water content in three different batches of the matrix. Results indicated that this biomaterial can absorb over 20 times its dried weight. The ash content of different batches of the matrix was always less than 0.1%. Finally, we used a solution of LBG before a cross-linking step, to test antioxidant activity of this material by ORAC assay. This assay determines the antioxidant potential of any

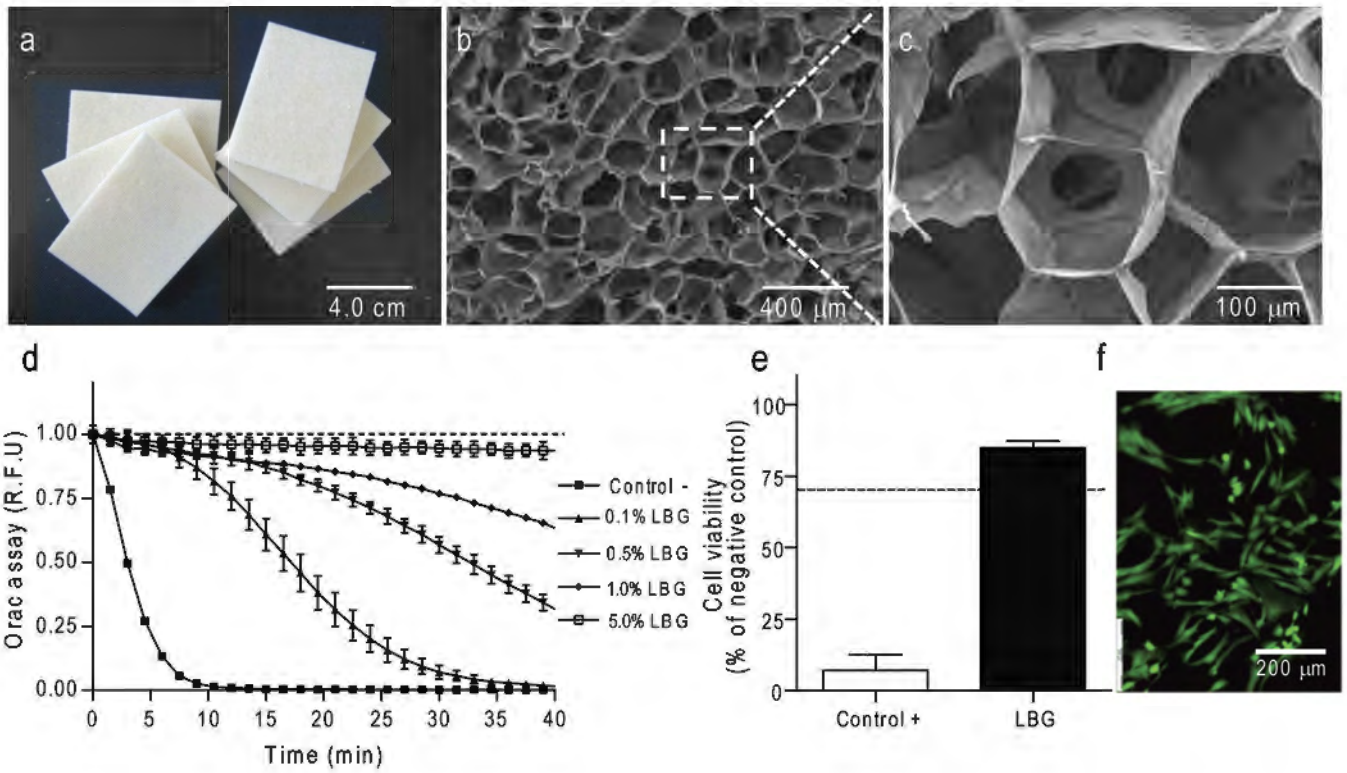

Fig. 1. Physico-chemical and biological characterization of HR006 matrix. Macro- and micro-images of the 3D lyophilized matrix **(a)** size 7×5 cm and **(b, c)** representative SEM images of the matrix at ×60 and ×250 magnification, respectively. **d.** Antioxidant activity of LBG as determined by ORAC assay. **e.** Cell viability of fibroblasts as determined by MTT assay when incubated with the matrix (dotted line represents the toxicity limit according to ISO 10993-5). **f.** Fluorescent microscopy analysis of cells stained with calcein AM on a 2D biofilm of LBG.

substance and biological sample. LBG showed good antioxidant activity in a dose-dependent manner that blocked nearly all oxidation of the fluorescent probe at ≥1% of LBG (Fig.1d).

To analyze the *in vitro* biological properties of the matrix, first lyophylized 3D matrix was used in a cytotoxicity assay. Results showed that the LBG matrix was not cytotoxic (Fig. 1e). Next, cell seeding behavior was analyzed on a 2D film of cross-linked LBG using calcein AM (Fig. 1f). Fibroblasts showed high viability and adhesion after 24 h in culture on this material adopting their typical spindle shaped cell morphology of fibroblasts.

Determination of the concentration of the components for the AH_{sol}

Different concentrations of curcumin and NAC were analyzed individually showing a high antioxidant activity (Fig. 2a,c). This activity was dose-dependent and almost fully blocked oxidation at concentrations of 100 μM curcumin and ≥1 mM NAC. We also used an *in vitro* cytotoxicity assay to determine the effects of curcumin and NAC on fibroblasts. Cell viability was evaluated at 24 h using MTT assay on treated fibroblasts (Fig. 2b,d). Curcumin concentrations of up to 5 μM did not affect cell viability, however, the highest concentration tested, 10 μM, had a cytotoxic effect since cell viability was lower than 70% (limit value established by ISO 10993-5) (Fig. 2b). All tested concentrations of NAC showed no cytotoxic effects on human fibroblasts (Fig. 2d). Based on ORAC assay and cytotoxicity results, the concentrations of 5 μM curcumin and 5 mM NAC were selected for the AH_{sol} of HR006.

AH_{sol} in vitro activity

Oxidative stress model using human fibroblasts

An oxidative stress model was established and characterized by incubating human fibroblasts with different concentrations of H_2O_2. Exposure of cells to 0.1, 0.25, 0.5, 1.0, and 1.5 mM of H_2O_2 showed a dose-dependent cytotoxic effect and a reduction in cell proliferation. After 24 h post-oxidation, cell viability was reduced 7.1%, 22.3%, 33.7%, 53.7%, and 79.9%, respectively. Regression analysis of the data gave an IC50 estimate of 0.97 mM. Microscopically, cells exposed to H_2O_2 showed progressive morphological

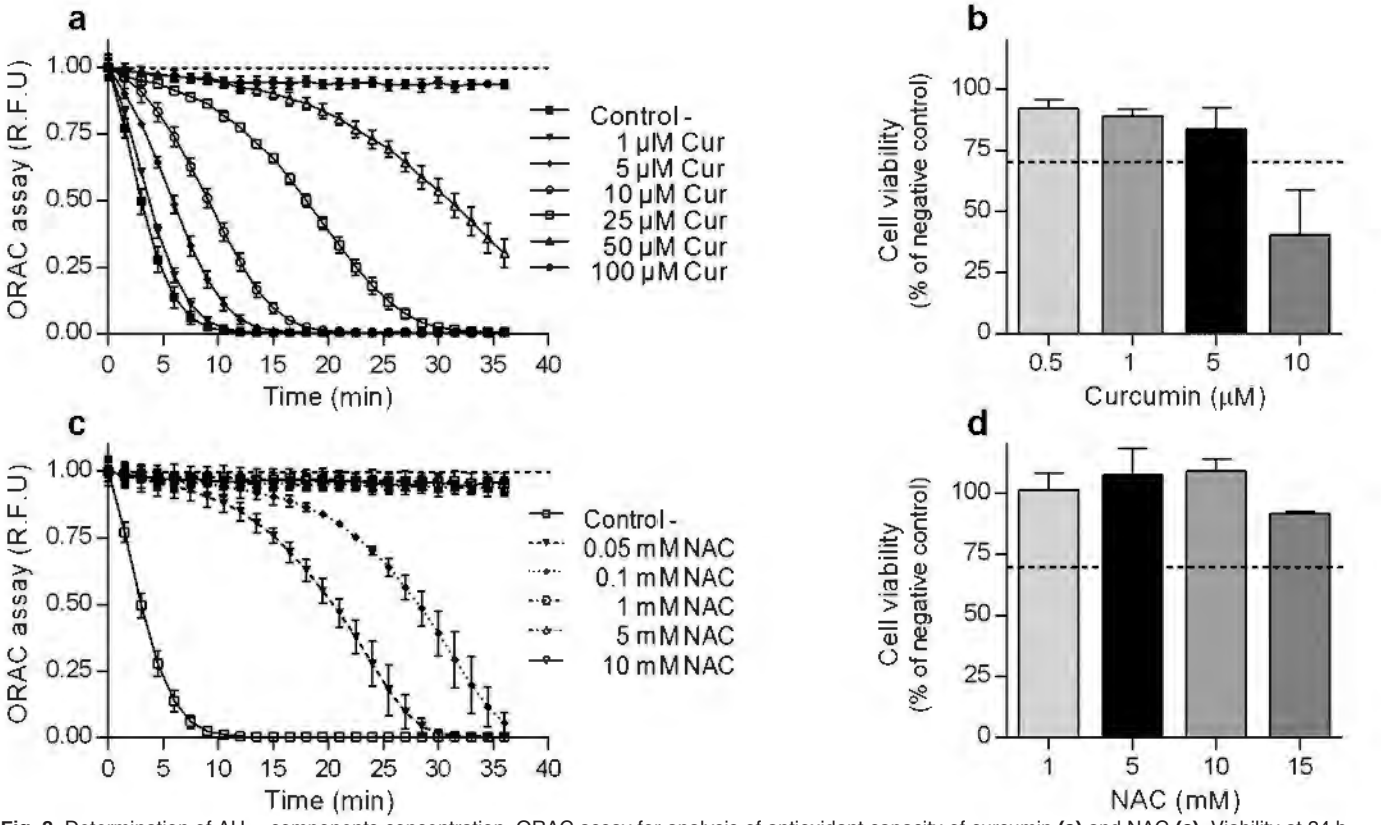

Fig. 2. Determination of AH_{sol} components concentration. ORAC assay for analysis of antioxidant capacity of curcumin **(a)** and NAC **(c)**. Viability at 24 h of human fibroblast treated with different concentrations of curcumin **(b)** and NAC **(d)**.

damage in a H_2O_2-concentration dependent manner (Fig. 3a-c). Cultures had enlarged pleiomorphic epithelioid fibroblasts, an arbitrary organization with no orientation pattern, and a degenerating fibroblast phenotype, especially at the highest concentrations of H_2O_2. Also, clear signs of senescence and detachment of cells from the surface of the culture plate were observed.

Analyses of intracellular ROS production at 30 min after fibroblast oxidation, demonstrated a fast dose-dependent increase in ROS (Fig. 3d). Simultaneously, as expected because GSH detoxifies ROS radicals, intracellular GSH concentrations decreased significantly in a dose-dependent manner (Fig. 3e). At the 30 min time point, ROS levels reached a plateau with 1.0 M H_2O_2, while GSH levels were reduced by a 32% of the control ($P<0.0001$). Interestingly, intracellular GSH reduction was only reversible when fibroblasts were oxidized with the lower concentrations of H_2O_2 (0.1 and 0.25 mM), recovering to near basal levels after 8 h. However, when cells were exposed to higher concentrations of H_2O_2 (0.5 and 1.0 mM), further declines of GSH up to 50% of the control were observed.

Effect of the AH_{sol} on oxidized fibroblasts

In an attempt to predict the potential benefits of the antioxidant activity of the AH_{sol} in wound healing, the effects of this solution in the H_2O_2 induced oxidative stress model of human fibroblasts were analyzed by measuring intracellular ROS production. Co-incubation of cells with the AH_{sol} significantly reduced intracellular ROS levels, both when using 0.25 or 1.0 mM concentrations of H_2O_2 (Fig. 4a). Furthermore, the AH_{sol} was also capable of preventing cell death due to oxidative stress, and oxidized AH_{sol} treated fibroblasts proliferated better than oxidized untreated controls (Fig. 4b).

To further elucidate the potential role of the AH_{sol} in indirectly modulating inflammation in the wound,

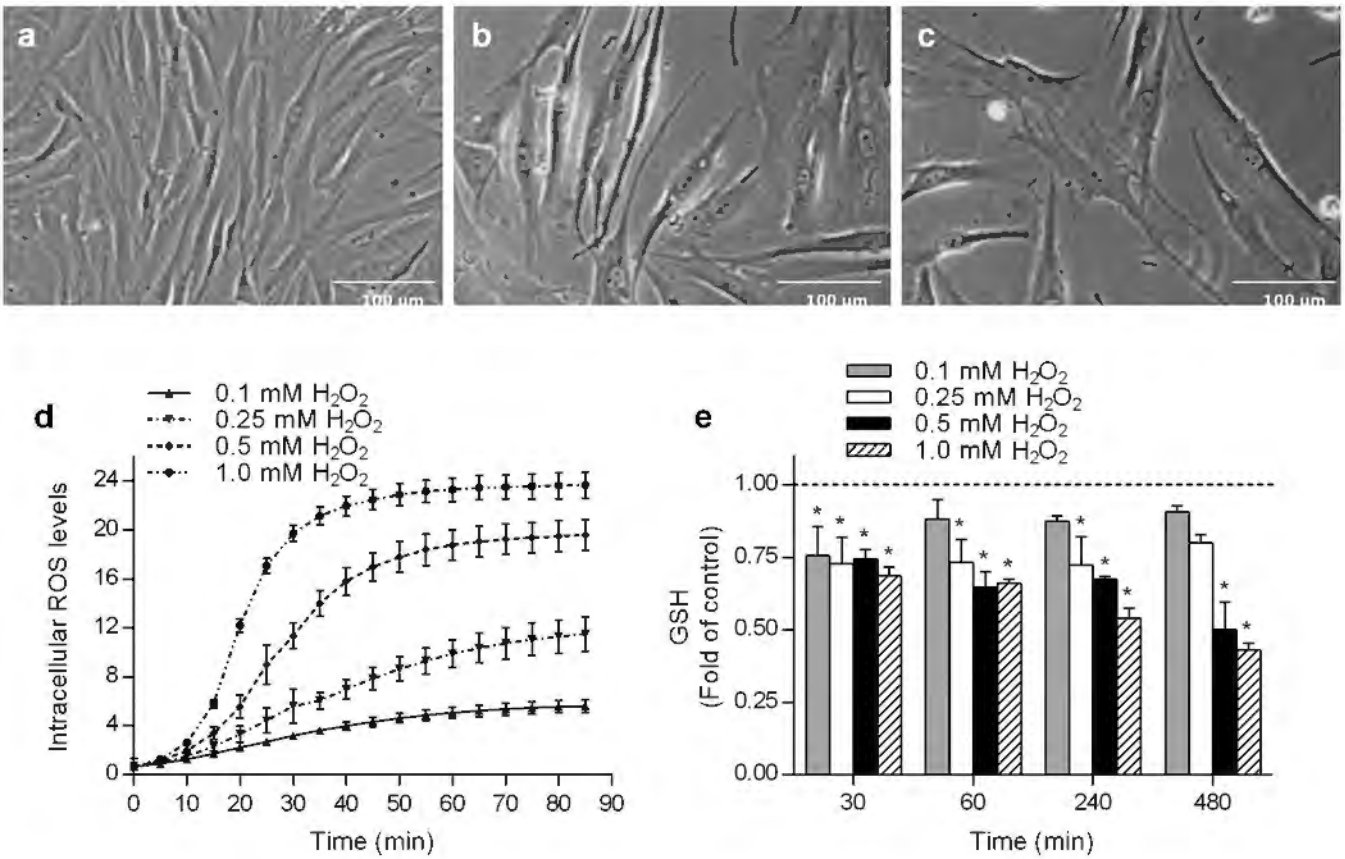

Fig. 3. Effects of oxidative stress in human fibroblasts using H_2O_2. **a-c.** Phase contrast microscopy images of human fibroblasts exposed to increasing concentrations of H_2O_2. Micrographs show a representative field of the control or H_2O_2 exposed cells: control **(a)**; 0.25 mM H_2O_2 **(b)**; 1.0 mM H_2O_2 **(c)**. Cells were oxidazed for 1 h and incubated in fresh media for 24 h before images were obtained. **d.** Intracellular ROS levels after exposure to different concentrations of H_2O_2. Data expressed as relative fluorescent units (RFU) using the DCFH-DA fluorescent probe. Fluorescence intensity is proportional to the amount of intracellular ROS. **e.** Intracellular GSH levels after exposure to H_2O_2; values expressed as relative to non-oxidized control cells. All experiments were repeated at least three times. (*) Significant differences with respect to the non-oxidized control ($P<0.05$).

relative expression of selected genes involved in inflammation and wound healing were estimated in *in vitro* oxidized and AH_{sol} treated fibroblasts using quantitative real time PCR. At 4 h after oxidative stress of fibroblast, higher levels of COX-2, TNF-α, IL-1α, IL-1β mRNA were detected in comparison to un-oxidized

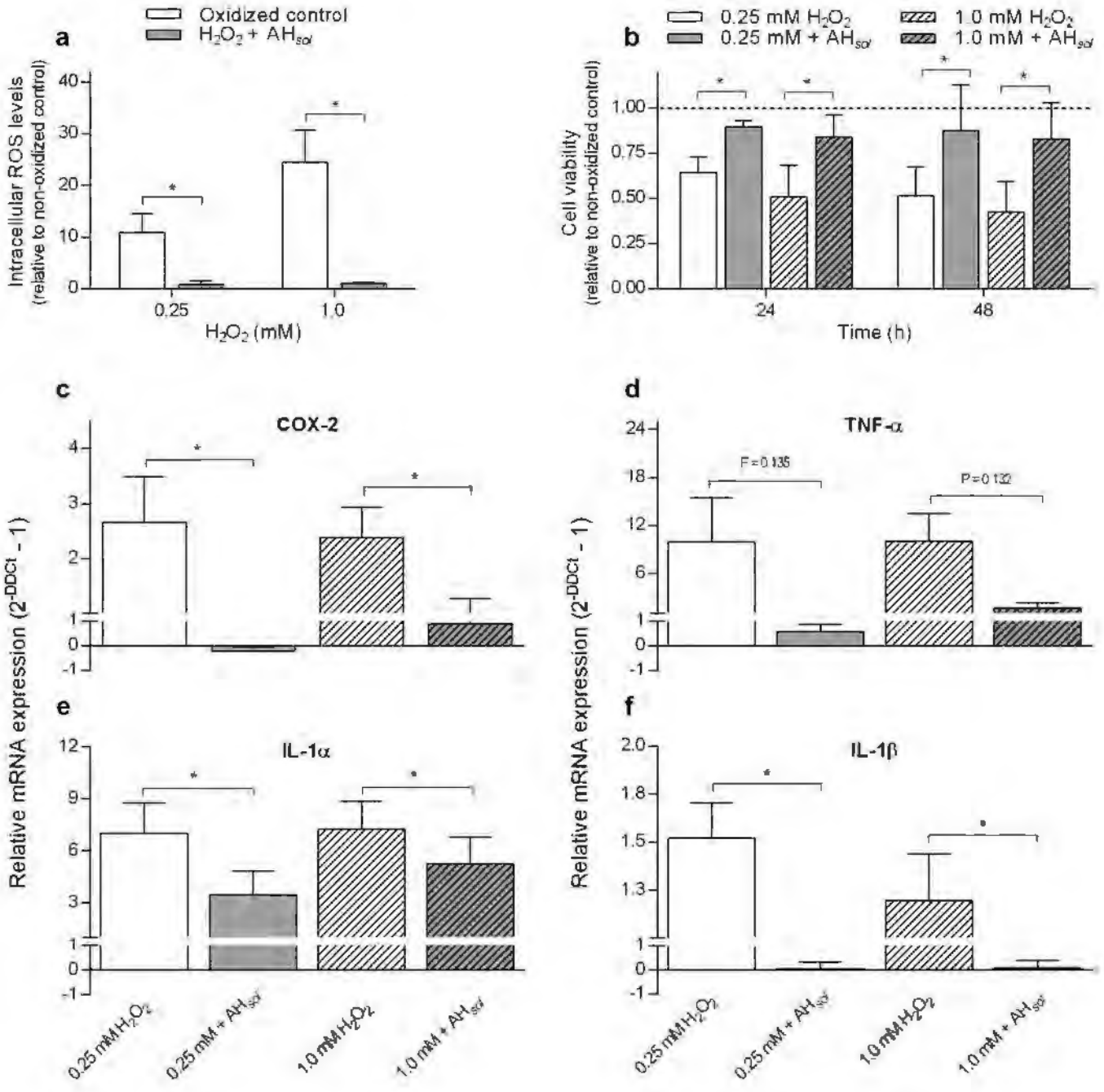

Fig. 4. Effects of AH_{sol} in prevention of oxidative stress. Human fibroblasts were exposed to H_2O_2 and the protective effect of AH_{sol} was analyzed by **(a)** intracellular ROS levels, cell proliferation **(b)**, and inflammatory genes expression **(c-f)** (COX2, TNF-α, IL-1α and IL-1β) measured by qPCR. Note that since fibroblasts' basal gene expression levels for TNF-α, IL-1α, and IL-1β were low, qPCRs were run using 10 times more cDNA than for COX-2. (*) Significant differences (P<0.05).

control cells (Fig. 4c-f). This overexpression was partially or totally reversed in the presence of AH_{sol} depending on the concentration of H_2O_2 used and the gene examined. At lower concentration of H_2O_2 (0.25 mM), fibroblasts simultaneously treated with AH_{sol} showed similar expression levels of COX-2 and IL-1β mRNA to those of un-oxidized control cells (Fig. 4c,f). TNF-α and IL-1α mRNA levels were also reduced in comparison to untreated oxidized cells (Fig. 4d,e). Furthermore, even at the very high and cell-damaging concentration of 1.0 mM H_2O_2, a statistically significant reduction in mRNA levels of COX-2, IL-1α, and IL-1β was observed (Fig. 4c,e,f).

Antioxidant effect and biocompatibility of HR006

Since one of the objectives of the new wound dressing was to exert an antioxidant effect during wound healing, we decided to test the intracellular ROS levels in the oxidative stress model in the presence of HR006

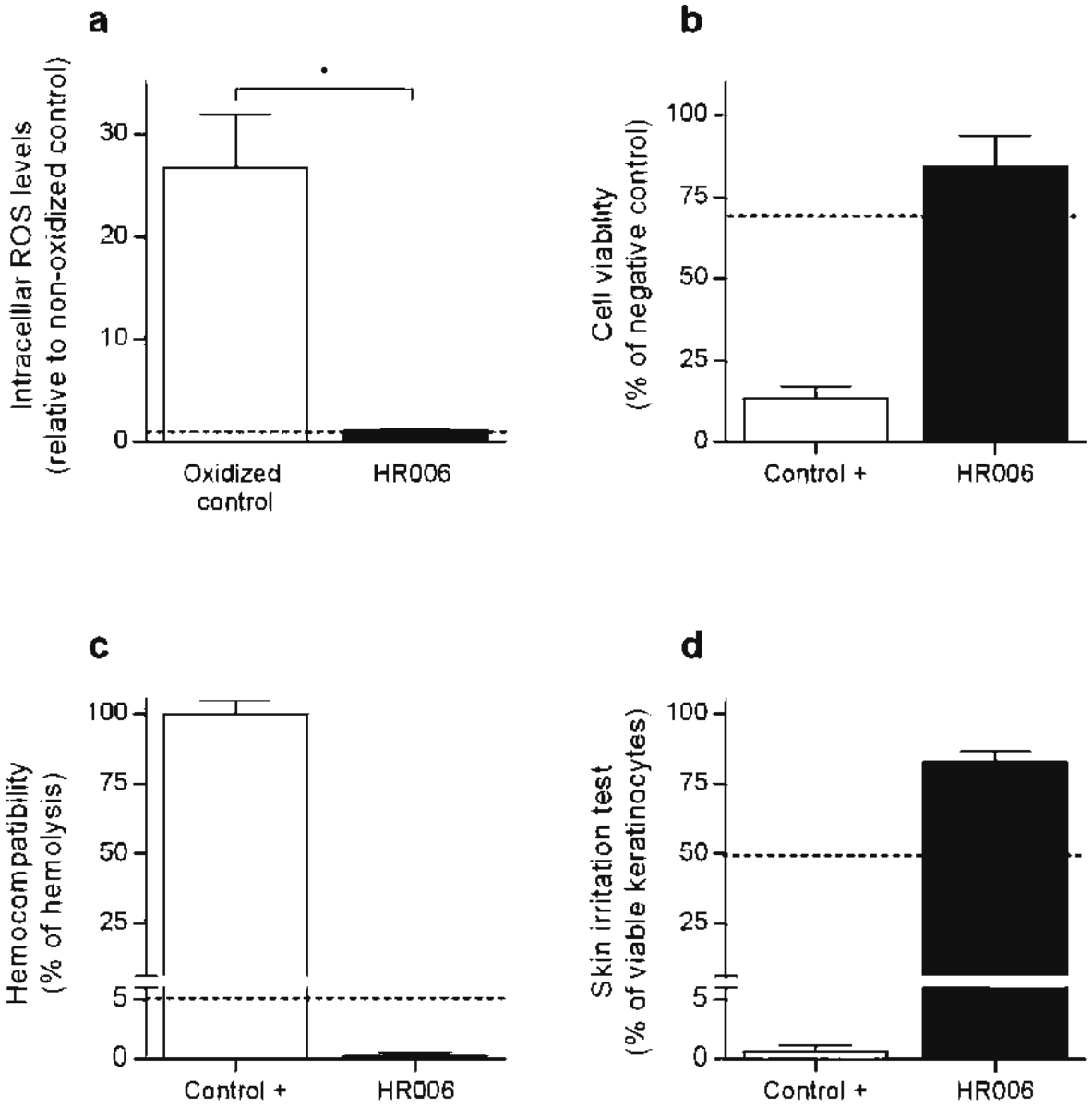

Fig. 5. Antioxidant and biocompatibility analyses of HR006. **a.** Intracellular ROS levels after oxidative stress induced in human fibroblasts with 1.0 mM H_2O_2 in the presence of HR006 components. **b.** L929 murine fibroblasts' viability after incubation with HR006 extracts. **c.** Percent hemolysis induced by HR006 extracts. **d.** *In vitro* skin irritation test, data are expressed as percent viability of skin keratinocytes (dotted line represents the limit of acceptance under ISO standards for each assay).

components. As can be seen in Fig. 5a, when cells were oxidized with 0.25 mM H_2O_2, HR006 almost fully inhibited intracellular ROS levels increase.

As stated by ISO Norm 10993, the study of the biocompatibility of a new medical device is an essential step in its development because these analyses determine whether a product can have any potential harmful physiological effects. Cytotoxicity of HR006 was analyzed using fluid extracts from the hydrated matrix (ISO 10993-5), and no effect on cell viability was observed (Fig. 5b). To evaluate the interaction of the product with blood, the effect of HR006 on erythrocyte membrane integrity was analyzed using a hemocompatibility test (ISO 10993-4). Percent of hemolysis over the positive control (1% solution of Triton x-100) was 0.3% for HR006 indicating no hemolytic activity (Fig. 5c). The skin irritation test is used to determine if a device or material could be a potential irritant, and we tested HR006 on an ECVAM validated skin irritation replacement test based on a reconstructed human epidermis. Results clearly showed that direct exposure to HR006 is not irritant, as cell viability was 82.8% when compared to the negative control, a value which is much higher than the reference limit (50%) indicated by the protocol (Fig. 5d).

In vivo efficacy of HR006

In order to assess *in vivo* the new wound dressing's performance in relation to the improvement in wound healing and the quality of new tissue formation, an excisional wound healing model in pigs was used. We monitored the healing process by assessing the rate of the wound closure as a function of time, as shown in Fig. 6. Macroscopic analyses of the wounds showed that control wounds healed much slower than HR006-treated wounds. In fact, a significant progressive reduction in wound area for HR006-treated wounds in comparison to control wounds (14.8 to 45.1% reduction at days 3 and 16, respectively) was found.

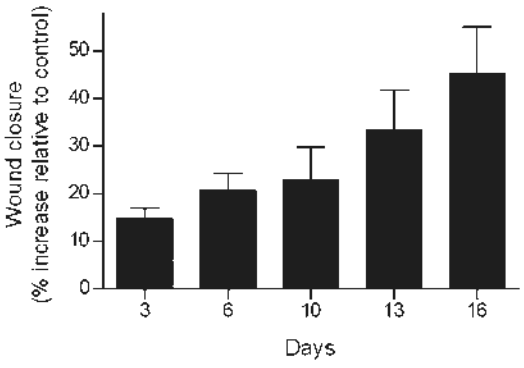

Fig. 6. Macroscopic analysis of wounds. Wound's evolution (days 0 to 16) expressed as percentage of increase of wound closure relative to control. Each data point represents the mean ± SEM of three pigs.

Histopathological analysis of the tissue sections of sequential wound biopsies at days 6, 10, and 16, obtained from 3 pigs, confirmed an accelerative effect of HR006 on wound healing with earlier granulation-tissue formation, neoangiogenesis, re-epithelization, and dermal remodeling. A more detailed histological analysis of a representative pig showed that at day 6 (Fig. 7a,d,g,j), which is near the end of the inflammatory phase of wound healing, HR006-treated wound tissue had fewer inflammatory cells and a higher number of fibroblasts than control wounds. This clearly indicates a tissue in transition from inflammatory into proliferative phase of wound healing. In addition, whereas an unresolved hemorrhagic region was still present in the control, initial neoangiogenesis –which is essential for the arrival of cells and nutrients to the wound and for cellular debris elimination– was also more advanced in HR006-treated wound. The re-epithelization bud on the control was trapped within this disorganized region, while HR006-treated wound showed a healthy re-epithelization edge that had already progressed and covered a relevant area of the wound.

Moving into day 10 (Fig. 7b,e,h,k), which would correspond to the proliferative or granulation tissue formation phases of wound healing, an enhanced fibroblast proliferation and neovascularization were observed in HR006-treated wound compared to the control. Also, many inflammatory cells were still present in control wound and not in HR006 sections, implying that HR006-treated wound had evolved much further than the control. In addition, larger deposits of extracellular matrix components and, in particular, collagen fiber deposition, were observed in HR006-treated wound. The highest speed of re-epithelization in HR006-treated sections seems to be guided by this new wound's extracellular matrix.

On day 16 sections (Fig. 7c,f,i,l), which should coincide with the remodeling phase of wound healing, HR006-treated wound showed a neoepidermis that was slightly thinner, but similar to a native epidermis with its corneal layer. In contrast, in control wound, the corneal layer was less apparent and organized. Moreover, the previously observed dermal inflammatory infiltrate had disappeared in HR006 treated wound, while in the control some inflammatory cells were still present. In this phase of tissue remodeling, in HR006-treated wound, granulation tissue started to involute, reducing the number of fibroblasts and blood vessels, and showing a more organized extracellular matrix, indentified by regular collagen orientation, when compared to control.

Discussion

A novel wound dressing for moist wound therapy was developed, characterized, and tested *in vitro* and in an animal wound healing model. HR006 is based on the combination of a galactomannan matrix and an AH_{sol} with antioxidant properties. LBG was optimal for the

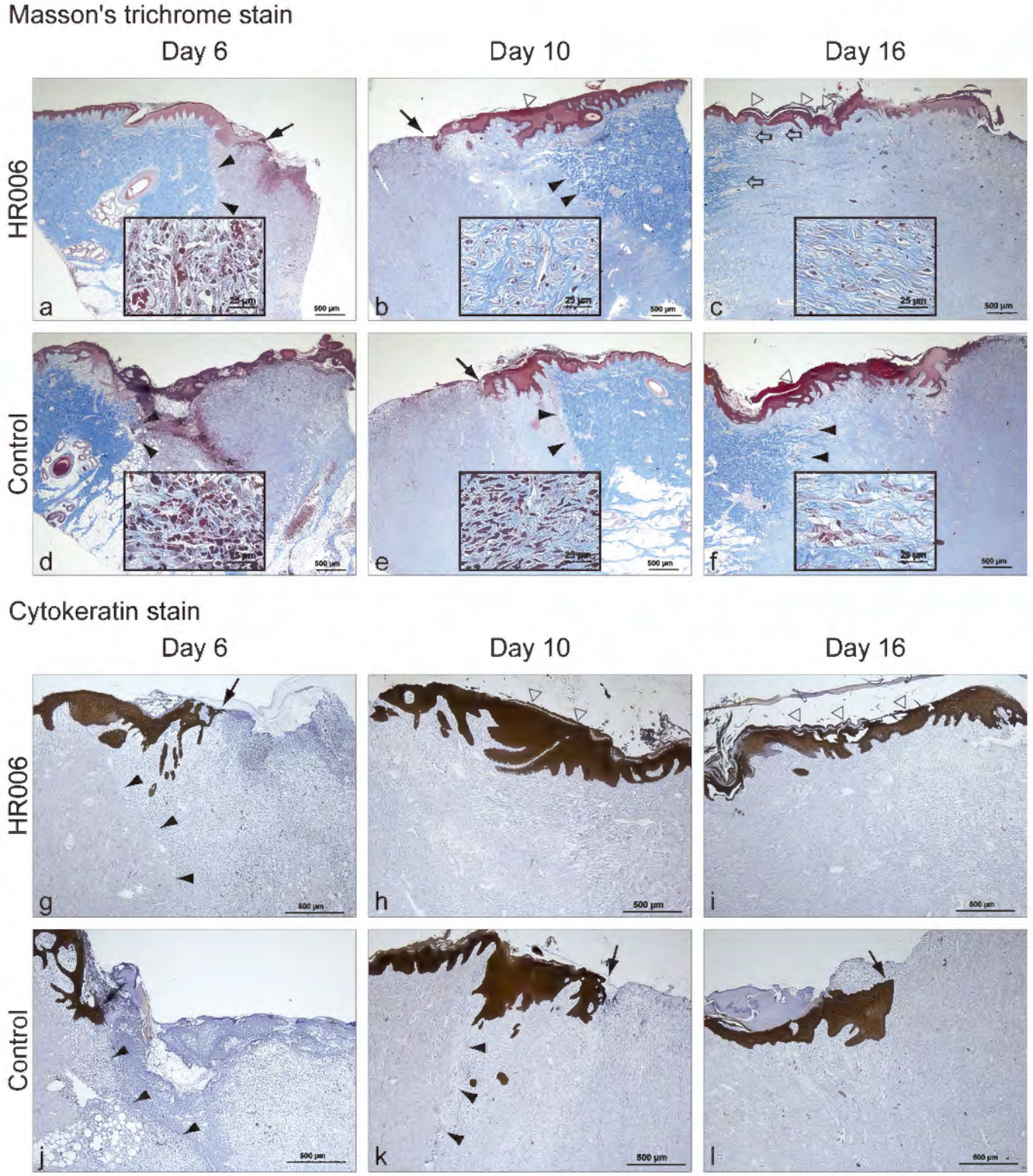

Fig. 7. Immunohistochemistry of wound tissue. Microscopic views of sections of HR006-treated and control wounds of a representative pig at 6, 10, and 16 days after surgery. **a-f.** Histological sections stained with Masson's trichrome stain. Zoomed images, inserts in the squared panels, correspond to a representative area of sections. **g-l.** Images of sections immunostained for wide spectrum cytokeratin: black arrowhead, demarcation line between healthy and wound tissue; *unresolved hemorrhagic region; black arrow, re-epithelization bud/edge; white arrow, collagen fibers; white arrowhead, corneal layer.

creation of a 3D hydrogel matrix with regular porosity and high liquid absorption capacity that would be beneficial in MWC. In addition, LBG was found to also have antioxidant activity, a fact that made it more appealing as a candidate for combination with the AH_{sol}. For this antioxidant solution, we decided to use curcumin because this compound has antioxidant and anti-inflammatory activities and has been used since ancient times due to its wound healing and dermal protective characteristics (Sidhu et al., 1998; Gupta et al., 2012; Gong et al., 2013; Hu et al., 2013; Akbik et al., 2014). We also included NAC, a GSH precursor, because of its good antioxidant properties, low toxicity, and synergistic activity with curcumin (Gillissen and Nowak, 1998; Morley et al., 2003; Kheradpezhouh et al., 2010).

The rationale behind this new product was that one of the main causes of delayed wound healing and chronification of wounds is the excessive production of ROS (Salim, 1991; Schäfer and Werner, 2008) that cannot be controlled by cells' internal mechanisms, such as GSH, create a toxic environment, a shift in redox equilibrium, and oxidative stress. All these interfere with the proper balance of inflammation and tissue remodeling processes that lead to wound closure (Gantwerker and Hom, 2012; Wagener et al., 2013).

We characterized an oxidative stress model with human fibroblasts to partially mimic conditions in the wound bed during healing and to test the antioxidant capabilities of the new wound dressing. Fibroblasts, which are the primary source of extracellular matrix components during wound healing, can be negatively affected by oxidative stress (Loo and Halliwell, 2012). To induce oxidative stress *in vitro*, we used different concentrations of H_2O. Intracellular ROS production in fibroblast was H_2O_2–dependant, and, as expected, cellular GSH levels were reduced through oxidation, all of these affect cell viability. Even at the concentration of 0.25 mM of H_2O_2, which is close to the physiological values present in wound exudates (Roy et al., 2006), a reduction in the number and a change in the phenotype of fibroblasts were observed. These changes could be due to the sensitivity of these cells to oxidative stress. In fact, the reduction of fibroblasts in the wound bed caused by oxidative stress is one of the reasons for the delay in wound healing (Loo and Halliwell, 2012).

The analysis of the effect of AH_{sol} components showed that both curcumin and NAC had good *in vitro* antioxidant capabilities as determined by the ORAC assay. We selected the concentrations of 5μM curcumin and 5mM NAC for the AH_{sol} of HR006 because, at these concentrations, the solution allowed cells to reduce intracellular ROS and come back to basal levels. In addition, while no toxicity was detected with any of the tested concentrations of NAC, in the case of curcumin the higher concentrations affected fibroblast viability, as other authors have previously shown (Lundviga et al., 2015). Incubation of fibroblasts with AH_{sol} during oxidative stress showed at 4 h a downregulation of mRNA expression of the inflammatory mediators COX-2, TNF-α, IL-1α, and IL-1β in comparison to oxidized control cells, suggesting that by neutralizing ROS present in the wound's exudate, HR006 could indeed modulate *in vivo* the inflammatory phase of wound healing, controlling excessive cell activation and allowing progression toward the proliferative and remodeling phases of wound healing. Other authors have described a similar modulation of these mediators of inflammation with equivalent concentrations of curcumin and NAC (Kim et al., 2000; Hu et al., 2013). Also, Kim et al. (2007) have previously shown that NAC is capable of neutralizing LPS induced ROS production and preventing increases in inflammatory cytokines IL-1β, IL-6, IL-8 and TNF-α and, more recently, Tsai et al. (2014) have demonstrated that topical NAC accelerates wound healing via the PKC/Stat3 pathway.

When AH_{sol} was combined with the LBG matrix, no cytotoxic effects were observed *in vitro*. Furthermore, HR006 showed good biocompatibility characteristics, having neither hemolytic nor skin irritation activities, all important characteristics of any new moist wound dressing (Rippon et al., 2012). The good results obtained *in vitro* prompted us to evaluate the *in vivo* efficacy of our dressing. We selected the excisional wound healing pig model (a surgical wound that removes the epidermis and dermis and reaches the hypodermis) because pig skin resembles much better human skin than that of any other animal (Winter, 1962; Jung et al., 2013).

Macroscopically, progression of wound healing was better for HR006-treated wounds in comparison to controls, and the differences, although evident from the early phases of wound healing, when higher inflammation and exudate levels occur, were maximal at the remodeling phase. Consistent with this observation, striking differences between treatments were observed in histological and immunostained sections. After hemostasis, the three main phases of wound healing involve inflammation (1-5 days), proliferation or granulation tissue formation (3-12 days) and remodeling or maturation (until day 21) (Gantwerker and Hom, 2012). Processes in these phases partially overlap, and bad wound care or other local and systemic factors can make a wound reverse to a previous phase or even become chronic. Overall in our experiments, histological and immunochemical-stained sections of HR006-treated wounds showed much better organized inflammatory tissue, which quickly gave way to an increased number of fibroblasts and an advanced and more organized synthesis of collagen and other components of the extracellular matrix (healthy granulation tissue). Moreover, HR006-treated wounds showed a faster and superior re-epithelization than control wounds.

We believe that early control of ROS excess by the new dressing might have been important and allowed a more controlled and organized healing process. The better and smoother inflammatory and granulation tissues observed in HR006-treated wounds, could be related to the *in vitro* observed reduction in

inflammatory genes expression. Thus, if the dressing managed to prevent ROS mediated expression of COX-2, as well as the release of pro-inflammatory cytokines TNF-α, IL-1α and IL-1β, as seen in the *in vitro* oxidative stress experiments, a more regulated and orchestrated inflammatory response might be the reason for the observed neoangiogenesis and early proliferation of fibroblasts in the repairing wound bed. These fibroblasts, not damaged because of the balanced control of ROS and inflammatory cytokines, might have been capable of dividing faster in the wound bed treated with HR006 than in the control. The better healing process observed at the microscopic level is easily illustrated by the fact that, for all sections and stains in Fig. 7, the broad histological image seen in HR006 sections corresponded to the wound healing phase of the next time point on the control sections.

In summary, the new wound dressing for moist wound therapy is biocompatible, flexible and porous, with high liquid absorption and retention capacity, maintaining a humidified environment in the wound. This antioxidant dressing has the potential to positively modulate important inflammatory and wound healing mediators and cytokines. Furthermore, HR006-treated wounds in pigs showed much better organization of tissues and faster re-epithelization in comparison to control wounds.

Acknowledgements. We want to thank Drs. Anna Puigdemont and Laura Ramio, from the Autonomous University of Barcelona for the help with the animal model experiments. We would also like to acknowledge General Research Services from the University of the Basque Country (SGIker, UPV/EHU). Partial funding for this project was provided by the Basque Government's Department of Industry, Innovation, Commerce, and Tourism (Spain) and the European Regional Development Fund under the program GAITEK. Additional funds were also obtained from the Spanish Center for Development of Industrial Technology (CDTI).
Conflicts of interest. All the authors, except JJ Soldevilla, have a relationship with the company that has an interest in the subject of this manuscript.

References

Akbik D., Ghadiri M., Chrzanowski W. and Rohanizadeh R. (2014). Curcumin as a wound healing agent. Life Sci. 116, 1-7.

Dreifke M.B., Jayasuriya A.A. and Jayasuriya A.C. (2015). Current wound healing procedures and potential care. Mater. Sci. Eng. C Mater. Biol. Appl. 48, 651-662.

Drew P., Posnett J. and Rusling L. (2007). The cost of wound care for a local population in England. Int. Wound J. 4, 149-155.

Finkel T. (2011). Signal transduction by reactive oxygen species. J. Cell Biol. 194, 7-15.

Fitzmaurice S.D., Sivamani R.K. and Isseroff R.R. (2011). Antioxidant therapies for wound healing: a clinical guide to currently commercially available products. Skin Pharmacol. Physiol. 24, 113-126.

Gantwerker E.A. and Hom D.B. (2012). Skin: histology and physiology of wound healing. Clin. Plast. Surg. 39, 85-97.

Gauron C., Rampon C., Bouzaffour M., Ipendey E., Teillon J., Volovitch M. and Vriz S. (2013). Sustained production of ROS triggers compensatory proliferation and is required for regeneration to proceed. Sci. Rep. 3, 2084.

Gillissen A. and Nowak D. (1998). Characterization of N-acetylcysteine and ambroxol in anti-oxidant therapy. Respir. Med. 92, 609-623.

Gong C., Wu Q., Wang Y., Zhang D., Luo F., Zhao X., Luo F, Zhao X., Wei Y. and Qian Z. (2013). A biodegradable hydrogel system containing curcumin encapsulated in micelles for cutaneous wound healing. Biomaterials 34, 6377-6387.

Günter C.I. and Machens H.G. (2012). New strategies in clinical care of skin wound healing. Eur. Surg. Res. 49, 16-23.

Gupta S.C., Patchva S., Koh W. and Aggarwal B.B. (2012). Discovery of curcumin, a component of golden spice, and its miraculous biological activities. Clin. Exp. Pharmacol. Physiol. 39, 283-299.

Hopman W.M., Buchanan M., Vandenkerkhof E.G. and Harrison M.B. (2013). Pain and health-related quality of life in people with chronic leg ulcers. Chronic Dis. Inj. Can. 33, 167-174.

Hu P., Huang P. and Chen M.W. (2013). Curcumin attenuates cyclooxygenase-2 expression via inhibition of the NF-κB pathway in lipopolysaccharide-stimulated human gingival fibroblasts. Cell. Biol. Int. 37, 443-448.

Jiang F., Zhang Y. and Dusting G.J. (2011). NADPH oxidase-mediated redox signaling: roles in cellular stress response, stress tolerance, and tissue repair. Pharmacol. Rev. 63, 218-242.

Jull A.B., Cullum N., Dumville J.C., Westby M.J., Deshpande S. and Walker N. (2015). Honey as a topical treatment for wounds. Cochrane Database Syst. Rev. 3, CD005083.

Jung Y., Son D., Kwon S., Kim J. and Han K. (2013). Experimental pig model of clinically relevant wound healing delay by intrinsic factors. Int. Wound J. 10, 295-305.

Kheradpezhouh E., Panjehshahin M.-R., Miri R., Javidnia K., Noorafshan A., Monabati A. and Dehpour A.R. (2010). Curcumin protects rats against acetaminophen-induced hepatorenal damages and shows synergistic activity with N-acetyl cysteine. Eur. J. Pharmacol. 628, 274-281.

Kim D.Y., Jun J.H., Lee H.L., Woo K.M., Ryoo H.M., Kim G.S., Baek J.H. and Han S.B. (2007). N-acetylcysteine prevents LPS-induced pro-inflammatory cytokines and MMP2 production in gingival fibroblasts. Arch. Pharm. Res. 30, 1283-1292.

Kim H., Seo J.Y., Roh K.H., Lim J.W. and Kim K.H. (2000). Suppression of NF-kappaB activation and cytokine production by N-acetylcysteine in pancreatic acinar cells. Free Radic. Biol. Med. 29, 674-683.

Kirsner R.S., Baquerizo Nole K.L., Fox J.D. and Liu S.N. (2015). Healing refractory venous ulcers: new treatments offer hope. J. Invest. Dermatol. 135, 19-23.

Loo A.E.K. and Halliwell B. (2012). Effects of hydrogen peroxide in a keratinocyte-fibroblast co-culture model of wound healing. Biochem. Biophys. Res. Commun. 423, 253-258.

Lundviga D.M.S., Pennings S.W.C., Brouwer K.M., Mtaya-Mlangwa M., Mugonzibwa E.A., Kuijpers-Jagtman A.M., Von den Hoff J.W. and Wagener F.A. (2015). Curcumin induces differential expression of cytoprotective enzymes but similar apoptotic responses in fibroblasts and myofibroblasts. Exp. Cell Res. 330, 429-441.

Morley N., Curnow A., Salter L., Campbell S. and Gould D. (2003). N-acetyl-L-cysteine prevents DNA damage induced by UVA, UVB and visible radiation in human fibroblasts. J. Photochem. Photobiol. B. 72, 55-60.

Murphy P.S. and Evans G.R.D. (2012). Advances in wound healing: a review of current wound healing products. Plast. Surg. Int. 2012, 190436.

Ou B., Hampsch-Woodill M. and Prior R.L. (2001). Development and validation of an improved oxygen radical absorbance capacity assay using fluorescein as the fluorescent probe. J. Agric. Food Chem. 49, 4619-4626.

Percival S.L., Bowler P. and Woods E.J. (2008). Assessing the effect of an antimicrobial wound dressing on biofilms. Wound Repair Regen. 16, 52-77.

Ray P.D., Huang B.W. and Tsuji Y. (2012). Reactive oxygen species (ROS) homeostasis and redox regulation in cellular signaling. Cell Signal. 24, 981-990.

Rippon M., Davies P. and White R. (2012). Taking the trauma out of wound care: the importance of undisturbed healing. J. Wound Care. 21, 359-368.

Roy S., Khanna S., Nallu K., Hunt T.K. and Sen C.K. (2006). Dermal wound healing is subject to redox control. Mol. Ther. 13, 211-220.

Salim A.S. (1991). The role of oxygen-derived free radicals in the management of venous (varicose) ulceration: a new approach. World J. Surg. 15, 264-269.

Schäfer M. and Werner S. (2008). Oxidative stress in normal and impaired wound repair. Pharmacol. Res. 58, 165-171.

Schreml S., Szeimies R.M., Prantl L., Landthaler M. and Babilas P. (2010). Wound healing in the 21st century. J. Am. Acad. Dermatol. 63, 866-881.

Sen C.K. and Roy S. (2008). Redox signals in wound healing. Biochim. Biophys. Acta 1780, 1348-1361.

Sen C.K. (2009). Wound healing essentials: let there be oxygen. Wound Repair Regen. 17, 1-18.

Sen C.K., Gordillo G.M., Roy S., Kirsner R., Lambert L., Hunt T.K., Gottrup F., Gurtner G.C. and Longaker M.T. (2009). Human skin wounds: a major and snowballing threat to public health and the economy. Wound Repair Regen. 17, 763-771.

Sidhu G.S., Singh A.K.., Thaloor D, Banaudha K.K., Patnaik G.K., Srimal R.C. and Maheshwari R.K. (1998). Enhancement of wound healing by curcumin in animals. Wound Repair Regen. 6, 167-177.

Smith M.E., Totten A., Hickam D.H., Fu R., Wasson N., Rahman B., Motu'apuaka M. and Saha S. (2013). Pressure Ulcer Treatment Strategies: a systematic comparative effectiveness review. Ann. Intern. Med. 159, 39-50.

Tsai M.L., Huang H.P., Hsu J.D., Lai Y.R., Hsiao Y.P., Lu F.J. and Chang H.R. (2014). Topical N-Acetylcysteine accelerates wound healing *in vitro* and *in vivo* via the PKC/Stat3 pathway. Int. J. Mol. Sci. 15, 7563-7578.

Tsala D.E., Amadou D. and Habtemariam S. (2013). Natural wound healing and bioactive natural products. Phytopharmacology 4, 532-560.

Vermeij W.P. and Backendorf C. (2010). Skin cornification proteins provide global link between ROS detoxification and cell migration during wound healing. PloS One 5, e11957.

Wagener F.A., Carels C.E. and Lundvig D.M.S. (2013). Targeting the redox balance in inflammatory skin conditions. Int. J. Mol. Sci. 14, 9126-9167.

Winter G.D. (1962). Formation of the scab and the rate of epithelization of superficial wounds in the skin of the young domestic pig. Nature. 193, 293-294.

Wolcott R.D., Rhoads D.D. and Dowd S.E. (2008). Biofilms and chronic wound inflammation. J. Wound Care 17, 333-341.

Accepted July 3, 2015